ELECTRONIC SUPPORTING INFORMATION (ESI)

Stable luminescent hybrid mesoporous copper complex-silica

Marisa Rico,[a] Angel E. Sepúlveda,[b] Santiago Ruiz,[b] Elena Serrano,[a] Jesús R. Berenguer*[b], Elena Lalinde[b] and Javier Garcia-Martinez*[a]

1. General methods

IR spectra were recorded on a Nicolet Nexus FT-IR Spectrometer. The spectra were taken with a 2 cm^{-1} resolution in a wavenumber range from 4000 to 200 cm^{-1}. All samples were prepared as Nujol mulls between polyethylene sheets and KBr pellets. NMR spectra were recorded on a Bruker ARX 400 spectrometer; chemical shifts are reported in ppm relative to external TMS (^{1}H and $^{13}C\{^1H\}$) or H_3PO_4 ($^{31}P\{^1H\}$), and coupling constants are given in Hz. Mass spectra were recorded on a micrOTOF-Q Bruker spectrometer. Diffuse reflectance UV-Vis (DRUV) data of pressed pure powder were recorded on a Shimadzu UV-3600 spectrophotometer with a Harrick praying mantis accessory, and recalculated following the Kubelka Munk function. Excitation and emission spectra were obtained on a Jobin-Yvon Horiba Fluorolog 3-11 Tau-3 spectrofluorimeter. The lifetime measurements were performed operating in the phosphorimeter mode (with an F1-1029 lifetime emission PMT assembly, using a 450 W Xe lamp). Quantum yields in the solid state were measured upon excitation at 400 nm for the grafted material (***G*-MSU_1**) and for the complex $[Cu(C{\equiv}CTol)(PPETS)]_4$ (**1**), and at 365 nm for the co-condensated hybrid materials (***IS*-MSU_1** and ***IS*-GEL_1**), using a F-3018 integrating sphere mounted in the Fluorolog 3-11 Tau-3 spectrofluorimeter. Data were fittered using the Jobin-Yvon software package. Elemental analyses of complex **1** were carried out with a Perkin-Elmer 2400 CHNS/O microanalyzer; while copper content in the hybrid materials was determined by ICP-AES on a Perkin Elmer 7300 DV spectrometer, with the samples dissolved in *aqua regia*, digested in a microwave and the undissolved siliceous matter filtered off prior to analysis.

The morphology of the mesoporous materials was investigated by transmission electron microscopy (TEM) using a JEM-2010 microscope (JEOL, 200 kV, 0.14 nm of resolution).

Samples for TEM studies were prepared by dipping a sonicated suspension of the sample in ethanol on a carbon-coated copper or gold grids for MSU-X sample (blank) and materials containing the copper complex, respectively. The digital analysis of the TEM micrographs was performed using DigitalMicrographTM 3.6.1. by Gatan.

Porous texture was characterized by N_2 adsorption at 77 K in an AUTOSORB-6 apparatus. The samples were previously degassed for 5 h at 373 K at 5×10^{-5} bars. BET surface area estimated by using multipoint BET method, using the adsorption data in the relative pressure (P/P_0) range of 0.05–0.30. The pore size distribution was calculated from the adsorption branch of the N_2 physisorption isotherms using the Barret-Joyner-Halenda (BJH) method.[1] As expected for these materials, the micropore volume, estimated from the t-plot method, was determined to be zero and thus the mesopore volume can be directly read from the isotherms at relative pressure of 0.95. These values are in good agreement with those obtained from the adsorption branch of the nitrogen isotherm using the BJH method, where the volume was measured at the plateau of the cumulative adsorption pore volume plot (approximately 40 nm).

$[Cu(C{\equiv}CTol)]_n$ was prepared according to literature procedures[2] and the rest of reagents were used as received without further purification.

2. Synthesis and characterization of $[Cu(C{\equiv}CTol)(PPETS)]_4$ 1 (PPETS = $PPh_2(CH_2)_2Si(OEt)_3$).

This reaction was carried out under argon atmosphere. To an anhydrous dichloromethane (15 mL) suspension of $[Cu(C{\equiv}CTol)]_n$ (0.125 g, 0.7 mmol) was added PPETS (251μL, 0.7 mmol) and the mixture was stirred at r.t. for 15 h. The yellow suspension was filtered to remove unreacted $[Cu(C{\equiv}CTol)]_n$ and a yellow solution was obtained, which was evaporated to dryness and was treated with Et_2O to afford the compound $[Cu(C{\equiv}CTol)(PPETS)]_4$ **1** as a yellow solid. Yield: 0.192 g (49%). **Elemental Anal. (%) Calcd. for $C_{116}H_{144}Cu_4O_{12}P_4Si_4$:** C, 62.74; H, 6.54. **Found:** C, 62.46; H, 6.67. **MS (ESI+)** *m*/*z* (%): 1957 [M - C≡CTol - 2 OEt - 2 Et]$^+$ (100). **IR** (ν_{max}/cm^{-1}): 3072m (C-H), 3051m (C-H), 3020m (C-H), 2972s (C-H), 2922s (C-H), 2883s

(C-H), 2049w (C≡C), 1898w (C≡C), 1587w (arom), 1571w (arom), 1503vs (arom), 1483m (C-H), 1434vs (P-C), 1409w, 1390m, 1266m, 1164s, 1077vs, 817s, 778s, 733s, 695vs, 510s, 482m, 462m, 222m (Cu-P), 214m (Cu-P). **^{1}H NMR** ($CDCl_3$) δ: At 223K: 7.8-6.8 (m, 40H, Ph); 7.30 (2H), 7.16 (2H), ≈ 6.9 (4H) (C_6H_4, signals overlap with the aromatic resonances due to phenyl groups, but have been observed and assigned by bidimensional heterocorrelations); 6.71 (d, $J_{H\text{-}H}$ = 8, 2H, C_6H_4); 6.58 (m, 4H, overlapping of two C_6H_4 doublets); 6.21 (d, $J_{H\text{-}H}$ = 7, 2H, C_6H_4); 3.84 (t, 3H), 3.68 (pst, 6H), 3.62 (t, 3H), 3.60 (t, 3H), 3.45 (pst, 6H), 3.29 (pst, 3H) (OCH_2CH_3); 2.44 (pst, J ≈ 13, 4H, P-CH_2); 2.39 (s, 3H), 2.36 (s, 3H), 2.30 (s, 3H) (CH_3, Tol); 2.24 (pst, J ≈ 13, 4H, P-CH_2); 2.11 (s, 3H, CH_3, Tol); 1.23 (t, 6H), 1.13 (t, 3H) (OCH_2CH_3); 1.15 (m, 4H, Si-CH_2, observed in HSQC); 1.01 (t, 9H, OCH_2CH_3); 0.96 (pt, 9H, OCH_2CH_3; 4H, Si-CH_2); 0.73 (t, 9H, OCH_2CH_3). At 298K: 7.8-6.8 (m, 40H, Ph); 7.39 (2H), 7.13 (2H) (C_6H_4, assigned by bidimensional heterocorrelations); 6.82 (2H), 6.72 (2H), (m br, C_6H_4); 6.54 (d, $J_{H\text{-}H}$ = 8, 4H, C_6H_4); 6.28 (d, $J_{H\text{-}H}$ = 8, 4H, C_6H_4); 3.6 (m br), 3.43 (m) (24H, OCH_2CH_3); 2.5-2.2 (m, 8H P-CH_2; 6H CH_3, Tol); 2.10 (s, 6H, CH_3, Tol); 1.20 (m, 9H, OCH_2CH_3); 1.17 (4H, Si-CH_2, observed in HSQC); 1.04 (m br, 9H, OCH_2CH_3); 1.03 (4H, Si-CH_2, observed in HSQC); 0.96 (t, 9H, OCH_2CH_3); 0.84 (m br, 9H, OCH_2CH_3). **^{13}C{^{1}H} NMR** ($CDCl_3$) δ: At 223K: 135.6, 135.4 (s, Ph); 135.1 (t, $^{1+3}J_{P\text{-}C}$ = 23, *i*-C, Ph); 135.0 (s, Ph); 134.3 (d, $J_{P\text{-}C}$ = 11.3, Ph); 134.1 (t, $^{1+3}J_{P\text{-}C}$ = 23, *i*-C, Ph); 133.5 (m, Ph); 133.2, 133.1 (s, C_6H_4); 132.5 (m, Ph); 132.3 (s br, Ph); 131.7 (s, Ph); 130.9, 130.3, 129.0 (s, C_6H_4); 128.5, 128.3 (s, Ph); 128.1 (s, C_6H_4); 128.0 (m, Ph); 127.9, 127.8 (s, C_6H_4); 126.2, 125.3, 124.1, 123.3, 122.6 (s, Ph); 118.1 (s, C_β); 107.4 (s br, C_α); 94.9 (d, $^{2}J_{P\text{-}C}$ ≈ 9, C_α); 93.2 (pst, $^{2}J_{P\text{-}C}$ ≈ 12, C_α); 83.5, 83.3 (s, C_β); 58.5, 58.0, 57.7 (s, OCH_2CH_3); 21.4, 21.2 (s, CH_3, Tol); 20.4 (pst, $^{1}J_{P\text{-}C}$ ≈ 10, P-CH_2); 19.8 (d, $^{1}J_{P\text{-}C}$ ≈ 13, P-CH_2); 18.0, 17.9 (s, OCH_2CH_3); 5.0, 4.7 (s, Si-CH_2). **^{31}P{^{1}H} NMR** ($CDCl_3$) δ: At 223 K: -1.5 (s br); -7.6 (s br). At 298 K: -1.2 (s br); -6.9 (br). The ^{1}H and ^{13}C{1H} NMR spectra, which have been assigned by homo- and heterobidimensional H-H (COSY) and H-C (HSQC, HMBC) correlations (see Experimental), show broad signals of difficult assignment at room temperature, while the presence of at least four non-equivalent acetylide and phosphine ligands are observed at 223 K.

This dynamic behaviour can be attributed to the lost of the molecule symmetry, the presence of reversible structural changes or partial degradation of the complex into dinuclear species. In fact, the relative intensity of the signals of 1 in the phosphorous or the proton spectra does not change with the addition of free PPETS to the NMR solutions; thus indicating the absence of phosphine dissociation in the dynamic processes.

3. Synthesis of the hybrid mesoporous materials

3.1. Synthesis of MSU-X (blank)

MSU-X silica material was prepared according to the procedure reported elsewhere.[3] In a typical synthesis, 0.58 g (0.9 mmol) of Triton X-100 (Aldrich), was magnetically stirred in 30 g of distilled water until a clear solution was obtained. Then, 3 mL of THF were added to 1.9 g of TEOS (9 mmol). This mixture was added dropwise to the solution of surfactant, being the two phases obtained vigorously for 15 minutes. To induce the silica precipitation, 3.4 ml of a solution 0.05 M of sodium fluoride (Aldrich, 99%) was added. The mixture was reacted at room temperature during 24 h under vigorous stirring. The obtained solid product was thoroughly washed (first with water and then with acetone), filtered off, and air dried overnight. Finally, the surfactant was removed by ethanol extraction (0.2 g catalyst / 50 ml ethanol) at room temperature for 12 h. FTIR spectra of silica materials after the surfactant extraction show only very weak intensity bands (C-H, 2987 cm^{-1}, 2924 cm^{-1}, 2863 cm^{-1}) due to the surfactant, thus confirming its practically quantitative extraction.[3,4] **IR** (ν_{max}/cm^{-1}): 3446m,br (O-H), 2987vw (C-H), 2924vw (C-H), 2863vw (C-H), 1633m, 1099vs,br (Si-O), 964m (Si-O), 801m (Si-O), 562w, 462s (Si-O).

3.2. Synthesis of *IS*-MSU_1

In a typical synthesis, 0.58 g (0.9 mmol) of Triton X-100 (Aldrich), was magnetically stirred in 30 g of distilled water until a clear solution was obtained. Then, a freshly prepared solution of 94 mg of $[Cu(C{\equiv}CTol)(PPETS)]_4$ **1** (0.04 mmol) in 3 mL of THF was immediately added to 1.9 g of TEOS (9 mmol, 1.7 wt% nominal $Cu:SiO_2$). This mixture was added dropwise to the solution of surfactant, being the two phases obtained vigorously stirred for 15 minutes. To induce the silica precipitation, 3.4 ml of a solution 0.05 M of sodium fluoride (Aldrich, 99%) was added. The mixture was reacted at room temperature during 24 h under vigorous stirring. The obtained solid product was thoroughly washed (first with water and then with acetone), filtered off, and air dried overnight. Finally, the surfactant was completely removed by ethanol extraction (0.2 g catalyst/50 ml ethanol) at room temperature for 12 h. **IR** (ν_{max}/cm^{-1}): 3428s,br (O-H), 2981m (C-H), 2929m (C-H), 2856w (C-H), 2019w (C≡C), 1896w (C≡C), 1633m, 1503w (arom), 1485w (C-H), 1438m (P-C), 1395w, 1082vs,br (Si-O), 959s (Si-O), 799s (Si-O), 695m, 543m, 459s (Si-O), 219w (Cu-P), 212w (Cu-P).

3.3. Synthesis of *G*-MSU_1

A similar MSU-X type silica to that previously reported as blank was the material used for the grafting incorporation of the copper complex. A freshly prepared solution of 94 mg of $[Cu(C\equiv CTol)(PPETS)]_4$ **1** (0.04 mmol) in 3mL of THF was added dropwise to a suspension of 0.53 g (9.0 mmol) of the pure mesoporous silica in 30 g of distilled water, being the two phases obtained vigorously stirred for 15 minutes. To induce the complex incorporation, 3.4 mL of a solution 0.05 M of sodium fluoride was added. The mixture was reacted at room temperature during 24 h under vigorous stirring. The obtained solid was washed with water, ethanol and acetone in succession, filtered off, and air dried. **IR** (ν_{max}/cm^{-1}): 3448m,br (O-H), 3074w (C-H), 3054w (C-H), 3020w (C-H), 2974w (C-H), 2924w (C-H), 2863w (C-H), 2019w (C≡C), 1896w (C≡C), 1637w, 1503w (arom), 1483w (C-H), 1436m (P-C), 1099vs,br (Si-O), 964m (Si-O), 801m (Si-O), 742w, 694m, 539sh, 467s (Si-O), 218w (Cu-P), 212w (Cu-P), 562w, 462s (Si-O). The TEM images showed some agglomerate onto the surface of the material obtained due to some extent self-condensation of the complex. Taking into account the low stability of complex **1** in aerobic solution, and in order to get a better diffusion of the precursor **1** molecules through the MSU-X type silica, suspensions of the pure mesoporous silica were stirred in anhydrous THF solution of **1** for more than 24 hours in several conditions (room temperature or reflux, with or without the presence of deoxygenated water) but no incorporation of the copper complex to the silica was observed in this conditions (reflux reactions with water yield the decomposition of the precursor **1**). Moreover, similar results were obtained when the same experiments were carried out adding catalytic amounts of *p*-toluenesulfonic acid after 12 hours of stirring. Chloridric acid was not considered as hydrolysis catalyst to avoid exchange reactions between the halide anions and the acetylide ligands.

3.4. Synthesis and characterization of *IS*-GEL_1

In order to test the influence of the surfactant (Triton X-100) in the preparation of the hybrid material ***IS*-MSU_1**, we have carried out the synthesis of a hybrid copper-silica gel following the same conditions to that employed for ***IS*-MSU_1**, but without using surfactant. Thus, a freshly prepared solution of 94 mg of $[Cu(C{\equiv}CTol)(PPETS)]_4$ **1** (0.04 mmol) in 3 mL of THF was immediately added to 1.9 g of TEOS (9 mmol, 1.7 wt% nominal $Cu:SiO_2$), and the mixture was added dropwise to 30 g of distilled water, being the two phases obtained vigorously stirred for 15 minutes. To induce the silica precipitation, 3.4 ml of a solution 0.05 M of sodium fluoride (Aldrich, 99%) was added. The mixture was reacted at room temperature during 24 h under vigorous stirring. The obtained solid product was washed with water, ethanol and acetone, filtered off, and air dried overnight. **IR** (ν_{max}/cm^{-1}): 3441s,br (O-H), 2982m (C-H), 2926m (C-H), 2854w (C-H), 2019w (C≡C), 1896w (C≡C), 1633m, 1504w (arom), 1485w (C-H), 1437m (P-C), 1408w, 1085vs,br (Si-O), 961s (Si-O), 798s (Si-O), 695m, 543m, 462s (Si-O), 222w (Cu-P), 213w (Cu-P). The photophysical data are included in Table S1.

As expected, the textural properties of the metal complex-containing material prepared without surfactant **(*IS*-GEL_1)** are significantly lower than that those prepared with surfactant by the *in-situ* methodology (***IS*-MSU_1**) (Figure S6). The nitrogen uptake at $P/P_0 = 0.5$ associated to the use of surfactant is not present in the case ***IS*-GEL_1** and its BET surface area is only 380 m^2/g while the surfactant-templated material (***IS*-MSU_1**) has a BET surface area of 600 m^2/g. Similarly, pore size distribution plot shows an average pore size around 17 nm for the ***IS*-GEL_1** which corresponds to interparticle porosity , instead of a pore size of 3,8 nm, as corresponds to the surfactant micelle size observed in both **MSU-X (blank)** and ***IS*-MSU_1** materials. Anyway, ***IS*-GEL_1** presents acceptable textural properties, similar to any other silica gel, proving that the methodology here in described to incorporate chemical functionality in the framework of porous supports can be extended to different porous material. The TEM micrographs of this material (Figure S7) confirm both the homogeneous metal complex incorporation (no dark spots are observed) and the wider porosity in comparison with the analogue material prepared by using surfactant.

The solid-state FT-IR and DRUV (Table S1) spectra show the incorporation of complex **1** to the structure of the hybrid material ***IS*-GEL_1**. In fact, the IR and DRUV profiles are nearly identical to those observed for ***IS*-MSU_1**. The textural properties of the hybrid materials seem also to have little influence in their emissive properties. Thus, ***IS*-GEL_1** presents, as ***IS*-MSU_1**, site selectivity emissive profiles, more clearly observed at low temperature (Table S1). Nevertheless, at room temperature, the observed emission maxima are slightly red-shifted and the efficiency of the emission is somewhat reduced (***IS*-GEL_1** $\phi \sim 0.04$ *vs.* ***IS*-MSU_1** $\phi \sim 0.10$).

Table S1: Photophysical data for 1, *IS*-MSU_1, *G*-MSU_1 and *IS*-GEL_1 in Solid State.

complex		DRUV (λ_{abs}/nm)	λ_{em}/nm (λ_{exc}/nm)	[$\tau/\mu s$] (λ_{em}/nm) {ϕ/%}
1	298 K	231, 325, 406	510 (325-460)	[11.1] (510) {93}
	77 K		510, 565*sh* (325-460)	[14.3] (510)
***IS*-MSU_1**	298 K	223, 261, 320	490 (365)	[59.4 (3%), 9.7 (97%)] (490) {11}
			476 (330)	
	77 K		493 (365)	[139.8 (38%), 26.0 (62%)] (500)
			454, 490 (330)	[139.2 (48%), 36.8 (52%)] (460)
***G*-MSU_1**	298 K	223, 264, 325, 407	512 (365-430)	[9.0] (510) {10}
	77 K		513 (365-430)	[11.5] (510)
***IS*-GEL_1**	298 K	222, 260, 323	500 (365)	[13.3 (24%), 4.0 (76%)] (500) {4}
			482 (330)	
	77 K		454sh, 482 (365)	[147.0 (29%), 28.8 (71%)] (480)
			454, 482 (330)	[90.2 (59%), 22.4 (41%)] (455)

Table S2: Photophysical data for suspensions of *IS*-MSU_1 in different solvents at room temperature.

solvent	λ_{em}/nm (λ_{exc} 330nm)	λ_{em}/nm (λ_{exc} 365nm)
H_2O	470	479
EtOH	470	479
Acetone	470	478
Acetonitrile	474	486
CH_2Cl_2	464	467

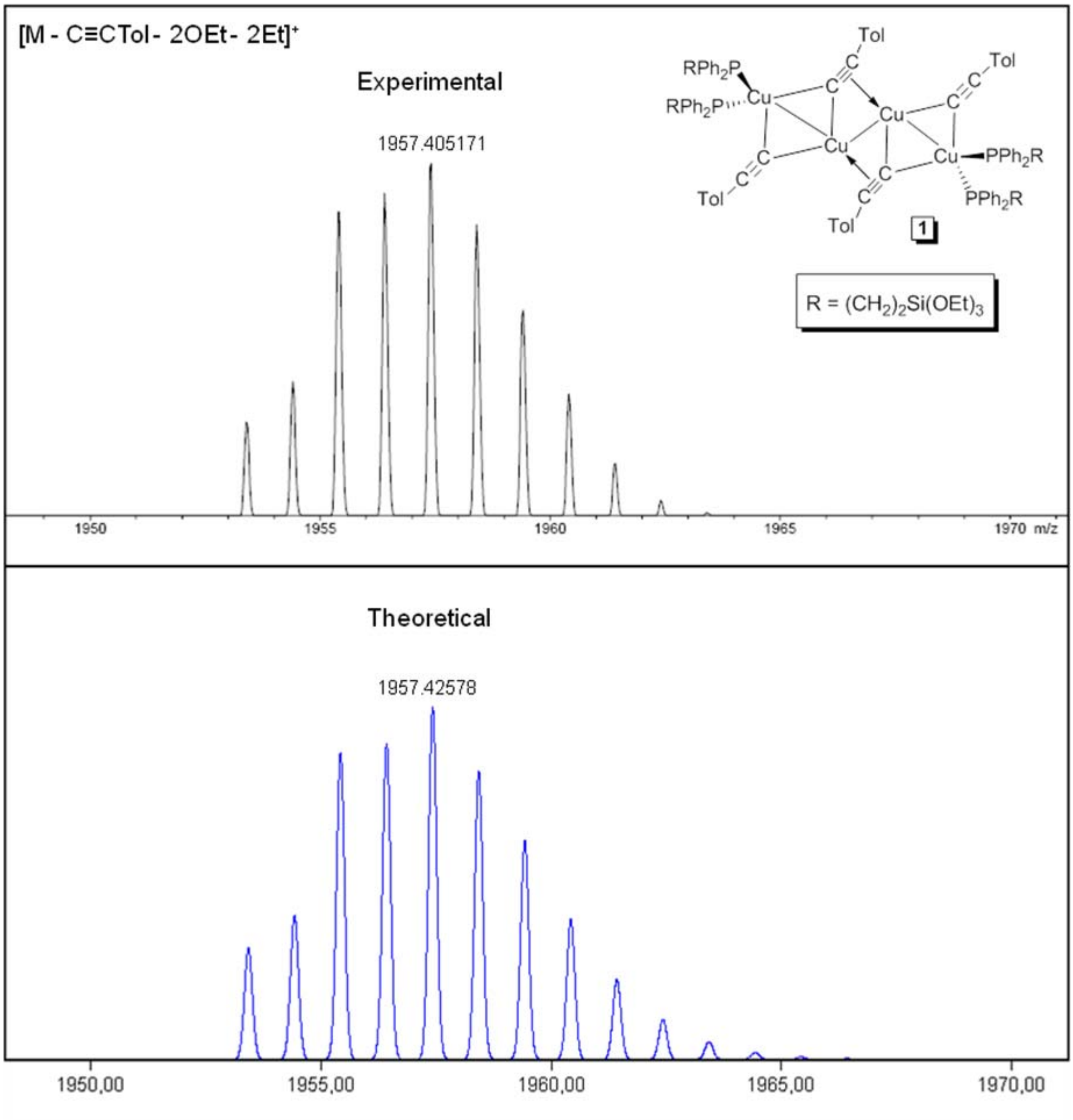

Figure S1. ESI+ Mass Spectrum spectrum of complex $[Cu(C\equiv CTol)(PPETS)]_4$ (**1**).

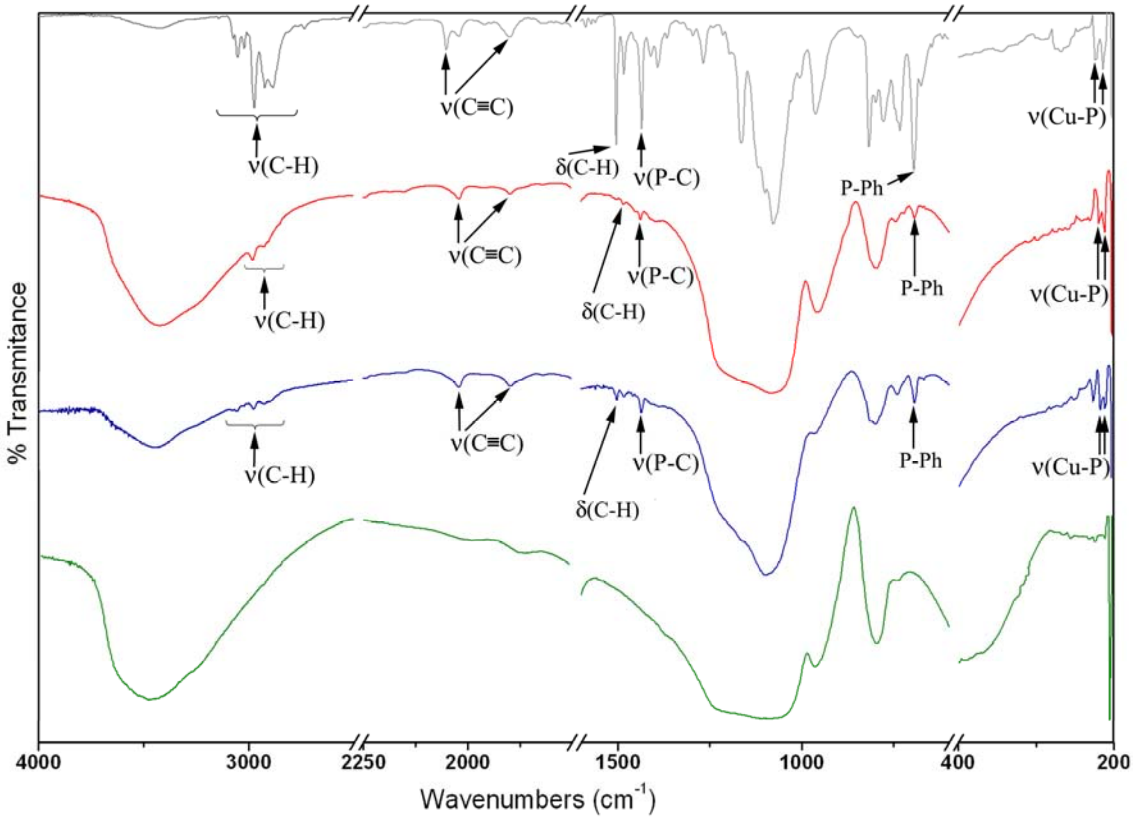

Figure S2. FTIR spectra of the as-synthesized materials: (a, top) complex $[Cu(C{\equiv}CTol)(PPETS)]_4$ (**1**), (b) MSU-X (blank), (c) *IS*-MSU_**1** and (d, bottom) *G*-MSU_**1**. The bands characteristics of the incorporation of the complex into the silica materials are denoted by arrows.

The FTIR spectra of the hybrid silica materials (IS-MSU_**1** and G-SU_**1**) show bands corresponding to the presence of phosphine and acetylide ligands at a similar frequency to those observed for the monomer complex **1**. Several absorptions are observed in the high energy region (3100-2850 cm^{-1}), characteristic of the ν(C-H) stretching vibration of the aromatic rings and the CH_2 units, [5] with a weak signal at ca. 1480 cm^{-1}, which can be assigned to δ(C-H) deformation vibration. [6] Also in the high energy region, two weak absorptions corresponding to the acetylide ligands (ν(C≡C)) appears at ca. 2030 and 1900 cm^{-1}. [7] Due to the phosphine ligand also appear a signal at ca. 1435 cm^{-1}, characteristic of the ν(P-C) stretching vibrations, [5] an intense absorption at 695 cm^{-1}, ascribed to the phenyl rings, and the two ν(Cu-P) bands observed at approximately 220 and 214 cm-1. [6]

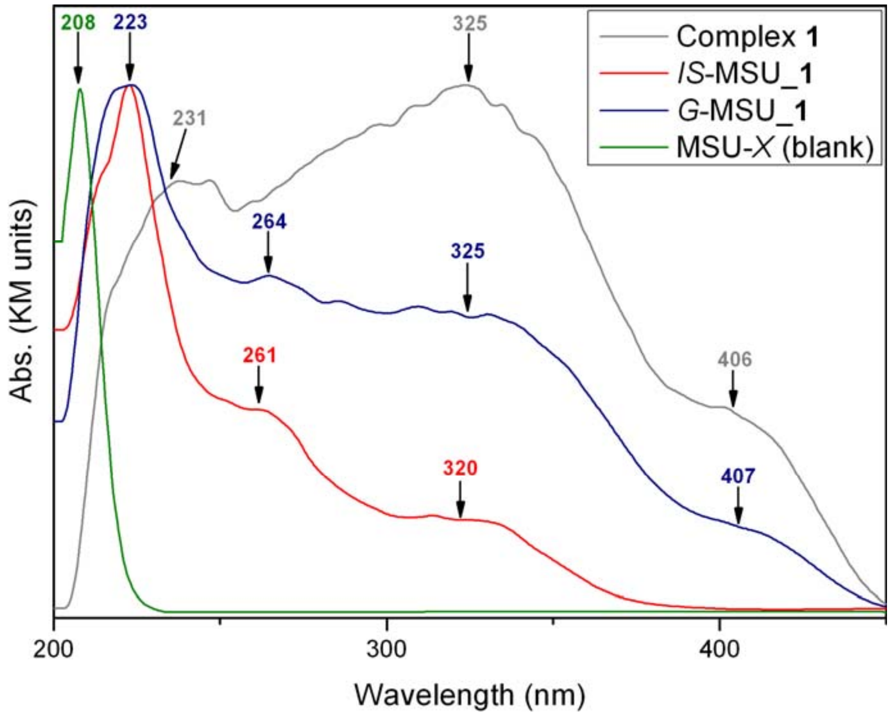

Figure S3. DRUV spectra of pressed pure powders of complex [Cu(C≡CTol)(PPETS)]$_4$ (**1**) and the copper-silica materials prepared by both the *in-situ* and grafting methods, as compared with the complex-free MSU type silica.

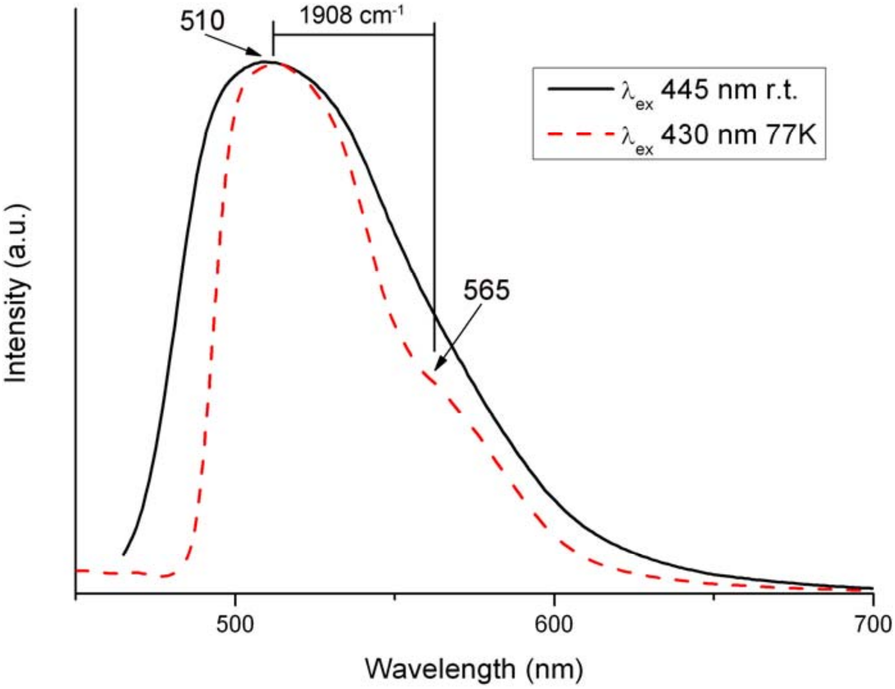

Figure S4. Emission spectra of complex [Cu(C≡CTol)(PPETS)]$_4$ (**1**) in solid state at room temperature and 77 K.

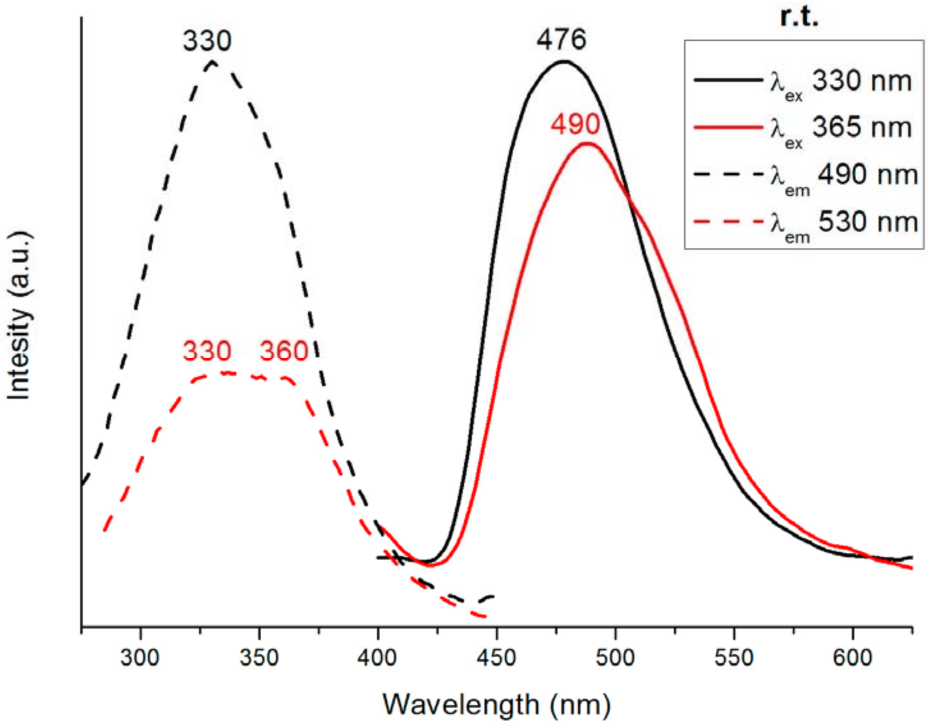

a

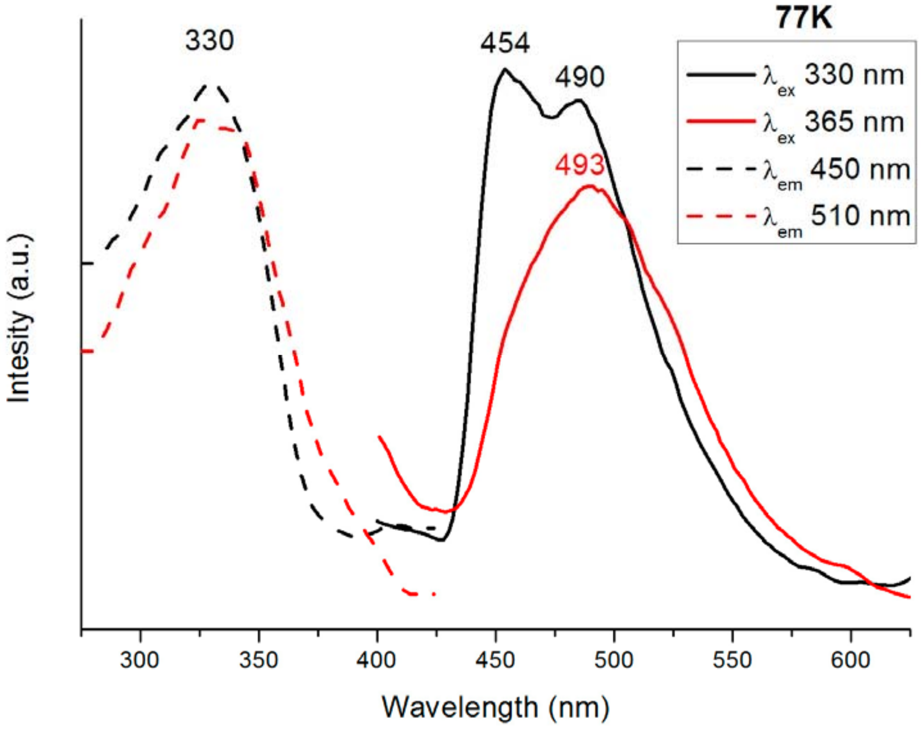

b

Figure S5. Emission spectra of the hybrid copper-silica material *IS*-MSU_**1** with excitation at different wavelengths at room temperature (a) and 77K (b).

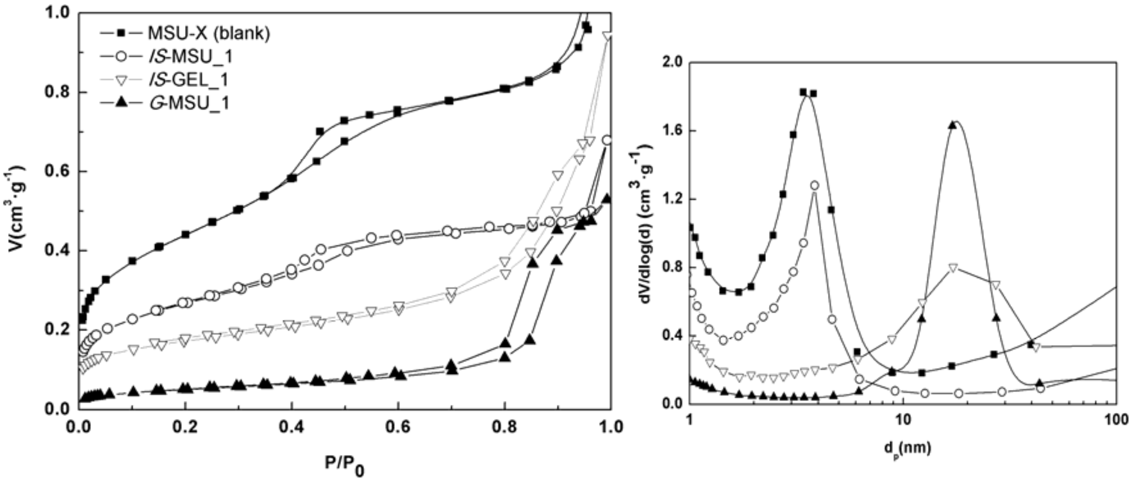

Figure S6. Representative nitrogen adsorption isotherms (left) and their corresponding pore size distribution (right) of the metal complex-containing material prepared without surfactant (*IS*-GEL_**1**) as compared to the solids prepared with surfactant and shown in Figure 1 of the manuscript.

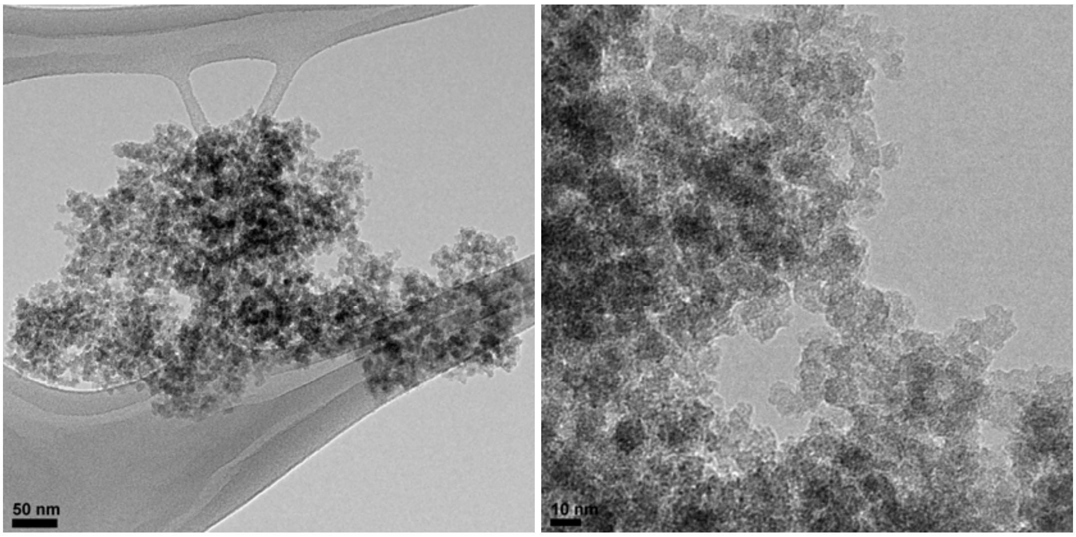

Figure S7. Representative TEM images of metal complex-containing material prepared without surfactant (*IS*-GEL_**1**) at two different magnifications (scale bar = 50 nm, left, and 10 nm, right).

References

[1] Rouquerol, F.; Rouquerol, J.; Sing, K. S. W., Adsorption by Powders and Porous Solids: Principles, Methodology and Applications; Academic Press: London, 1999.

[2] Van Koten, G.; Noltes, J. G. In *Comprehensive Organometallic Chemistry*; Wilkinson, G., Stone, F. G. A., Lebel, E., Eds.; Pergamon Press, Oxford, 1982; Vol. 2, p 720.

[3] N. Linares, A.E. Sepulveda, M.C. Pacheco, J.R. Berenguer, E. Lalinde, C. Najera and J. Garcia-Martinez, *New J. Chem.,* 2011, **35**, 225.

[4] N. Kimura, J. Umemura, S. Hayashi, *J. Colloid Int. Sci*., 1996, **182**, 356.

[5] X. Yang, F. Zhu, J. Huang, F. Zhang, H. Li, *Chem. Mater*., 2009, **21**, 4925.

[6] K. Nakamoto, in Infrared and Raman Spectra of Inorganic and Coordination Compounds. Part B Applications in Coordination, Organometallic, and Bioinorganic Chemistry, John Wiley & Sons Inc., New Jersey, 6th edn. 2009.

[7] W. H. Chan, Z. Z. Zhang, T. C. W. Mak, C. M. Chem, *J. Organomet. Chem.* 1998, **556**, 169.